

A Mo(V) Monophosphate with a Chain-Like Structure: $\text{Ba}_3\text{Mo}_2\text{O}_2(\text{PO}_4)_4$

S. Ledain, A. Leclaire, M. M. Borel, J. Provost, and B. Raveau

Laboratoire CRISMAT, CNRS URA 1318, ISMRA et Université de Caen, Bd du Maréchal Juin, 14050 Caen Cedex, France

Received February 20, 1996; in revised form May 1, 1996; accepted May 9, 1996

A pentavalent molybdenum monophosphate $\text{Ba}_3\text{Mo}_2\text{O}_2(\text{PO}_4)_4$, with a chain like-structure has been synthesized for the first time. It crystallizes in the $P\bar{1}$ space group with $a = 4.822(1)$ Å, $b = 9.189(1)$ Å, $c = 17.948(2)$ Å, $\alpha = 87.69(1)^\circ$, $\beta = 88.11(1)^\circ$, and $\gamma = 78.35(1)^\circ$. The structure consists of $[\text{Mo}_2\text{P}_4\text{O}_{18}]_\infty$ ribbons built up of corner-sharing PO_4 tetrahedra and MoO_6 octahedra running along a , whose cohesion is ensured by Ba^{2+} cations. Though there exist two kinds of ribbons, their geometry is very similar and they can be considered as practically enantiomorphic. The similarity of these ribbons with the layer structures of the phosphates $\text{ASb}(\text{PO}_4)_2$ and $\text{BaMo}(\text{PO}_4)_2$ is emphasized. In these chains, the MoO_6 octahedra have one free apex, whereas the PO_4 tetrahedra exhibit either one free or two free apices. © 1996 Academic Press, Inc.

INTRODUCTION

The exploration of transition metal phosphates performed these past 15 years has shown that the association of PO_4 tetrahedra with MoO_6 octahedra allows pentavalent molybdenum to be stabilized, leading to the generation of a large number of molybdenum (V) phosphates with an original structure (see for review Ref. 1–2).

Most of the thirty new Mo(V) phosphates that are known are characterized by a tridimensional framework, built up from corner- (or edge-) sharing MoO_6 octahedra and PO_4 tetrahedra, forming either tunnels or cages. Only two of them, α - $\text{CsMo}_2\text{O}(\text{PO}_4)_3$ (3) and $\text{BaMo}_4\text{O}_8(\text{PO}_4)_2$ (4), exhibit a layer structure. No Mo(V) phosphate with a unidimensional structure has been synthesized to date.

The existence of $\text{BaMo}_4\text{O}_8(\text{PO}_4)_2$ (4), with a bidimensional structure, suggests that barium may be a good candidate for the stabilization of Mo(V) phosphates with a chain-like structure. The synthesis of such a material should require a large amount of barium in order to ensure the connection between “Mo–P” chains. For this reason we have investigated the barium rich side of the Ba–Mo–P–O system, keeping formally molybdenum in the pentavalent state for the different explored compositions. We report herein on a new Mo(V) monophosphate $\text{Ba}_3\text{Mo}_2\text{O}_2(\text{PO}_4)_4$ with an original unidimensional structure.

SYNTHESIS AND CRYSTAL GROWTH

The synthesis of this new phase was performed in two steps. First an adequate mixture of MoO_3 , BaCO_3 , and $\text{H}(\text{NH}_4)_2\text{PO}_4$ was heated in air up to 673 K to eliminate CO_2 , NH_3 , and H_2O . In the second step the required amount of molybdenum was added and the mixture was heated at 1023 K for 12 hr. Under these conditions a pure phase was obtained in the form of a polycrystalline sample, whose powder X-ray diffraction pattern was indexed in a triclinic cell (Table 1) with the cell parameters deduced from the single crystal X-ray study (Table 2).

The growth of single crystals of this phosphate required the addition of lithium. It was carried out in two steps from a mixture of nominal composition $\text{Li}_{0.5}\text{Ba}_{0.5}\text{MoPO}_5$. First $\text{H}(\text{NH}_4)_2\text{PO}_4$, MoO_3 , Li_2CO_3 , and BaCO_3 were mixed in an agate mortar in adequate ratios and heated in air up to 673 K to eliminate CO_2 , NH_3 , and H_2O . In a second step, the appropriate amount of molybdenum was added and the finely ground mixture was placed in an alumina tube, sealed in an evacuated silica ampoule, and then heated for 18 hr at 973 K, cooled at 5 K per hr down to 773 K, and finally quenched to room temperature.

In the resulting mixture the major phase occurred as black powder with a minor phase of yellow crystals. The microprobe analysis of these yellow crystals leads to Mo/P/Ba ratios in agreement with the formula $\text{Ba}_3\text{Mo}_2\text{P}_4\text{O}_{18}$ deduced from the structure determination.

STRUCTURE DETERMINATION

A yellow crystal with dimensions $0.154 \times 0.051 \times 0.012$ mm³ was selected for the structure determination. The cell parameters were determined by diffractometric techniques at 294 K with a least square refinement based upon 25 reflections with $18^\circ < \theta < 22^\circ$. The data were collected with a CAD4 Enraf Nonius diffractometer with the parameters reported in Table 2. The reflections were corrected for Lorentz and polarization effects. The structure was solved with the heavy atom method. The refinement of the atomic parameters and the anisotropic thermal factors for Mo, P,

TABLE 1
X-Ray Powder Diffraction Data of Ba₃Mo₂O₂(PO₄)₄

<i>h</i>	<i>k</i>	<i>l</i>	<i>d</i> _{obs} (Å)	<i>d</i> _{calc} (Å)	<i>I</i>
0	1	-2	6.243	6.243	2.5
1	1	1	4.476	4.479	28
0	1	4	4.066	4.068	100
0	1	-4	3.953	3.958	98
1	-1	1	3.788	3.790	33
1	2	1	3.607	3.603	6.5
0	2	-3	3.533	3.536	34.5
1	2	2	3.428	3.431	20
1	-1	3	3.257	3.259	22
0	2	4	3.227	3.230	17
1	2	3	3.179	3.178	7.5
0	2	-4	3.122	3.121	8
1	2	-3	3.047	3.047	24
1	-1	4	2.938	2.939	10
1	2	4	2.893	2.894	44.5
0	1	6	2.869	2.865	86
1	0	-5	2.820	2.821	80
1	-2	-3	2.667	2.668	27
1	-1	-5	2.623	2.623	6.5
1	3	3	2.581	2.581	51
0	3	4	2.532	2.532	2.5
1	2	-5	2.497	2.497	7.5
1	0	-6	2.496		
0	2	-6	2.451	2.450	10.7
1	-1	-6	2.357	2.359	6.5
1	-3	-1	2.313	2.313	11.5
2	2	-1	2.257	2.257	15
1	0	-7	2.228	2.228	25
0	4	-1	2.223	2.222	21.5
0	4	2	2.199	2.199	16
1	4	-1	2.181	2.181	30.5
1	2	7	2.144	2.143	13
0	4	3	2.129	2.129	10
2	0	4	2.111	2.111	22.5
0	4	4	2.038	2.038	23
1	3	-6	1.996	1.996	13
2	0	5	1.995		
0	3	7	1.981	1.981	21
0	4	5	1.935	1.935	12
1	3	7	1.935		
2	-2	2	1.896	1.895	7
2	-1	5	1.872	1.874	55.5
1	-4	1	1.874		
1	1	9	1.855	1.855	12
1	3	-7	1.847	1.846	12
0	3	8	1.825	1.826	19

Ba, and O atoms were successful in the space group $P\bar{1}$ and led to the formulation Ba₃Mo₂O₂(PO₄)₄ with $R = 0.033$ and $R_w = 0.031$ and to the atomic parameters of Table 3.

DESCRIPTION OF THE STRUCTURE AND DISCUSSION

The projection of the structure along **a** (Fig. 1) shows its unidimensional character. It consists indeed of [Mo₂P₄O₁₈]_∞ ribbons running along **a**, whose cohesion is ensured through Ba²⁺ cations. The [Mo₂P₄O₁₈]_∞ ribbons are displayed in layers parallel to (001) as shown from the projection of the structure along **b** (Fig. 2). Although

TABLE 2
Summary of Crystal Data, Intensity Measurements, and Structure Refinement Parameters for Ba₃Mo₂O₂(PO₄)₄

1. Crystal data	
Space group	$P\bar{1}$
Cell dimensions	$a = 4.8222(6)$ Å $\alpha = 87.695(7)^\circ$ $b = 9.1896(7)$ Å $\beta = 88.110(9)^\circ$ $c = 17.948(2)$ Å $\gamma = 78.354(8)^\circ$
Volume (Å ³)	778.1(1) Å ³
<i>Z</i>	2
ρ_{calc} (gcm ⁻³)	4.335
2. Intensity measurements	
λ (MoK α)	0.71073
Scan mode	ω - θ
Scan width (°)	1.0 + 0.35 tan θ
Slit aperture (mm)	1.0 + tan θ
max θ (°)	45
Standard reflections	3 measured every 3600 s
Measured reflections	13064
Reflections with $I > 3\sigma$	3679
μ (mm ⁻¹)	9.56
3. Structure solution and refinement	
Parameters refined	244
Agreement factors	$R = 0.033$ $R_w = 0.031$
Weighting scheme	$w = 1/\sigma$
Δ/σ max	<0.005

TABLE 3
Positional Parameters and Their Estimated Standard Deviations in Ba₃Mo₂O₂(PO₄)₄

Atom	<i>x</i>	<i>y</i>	<i>z</i>	<i>B</i> (Å ²)
Ba(1)	0.2205(1)	0.00398(6)	0.25183(3)	0.792(8)
Ba(2)	0.5357(1)	0.40935(7)	0.34574(3)	0.840(8)
Ba(3)	0.9035(1)	0.59757(7)	0.14637(3)	0.808(8)
Mo(1)	0.3060(1)	0.76406(8)	0.44883(4)	0.44(2)
Mo(2)	0.1719(2)	0.22754(8)	0.05021(4)	0.41(2)
P(1)	0.2971(5)	0.8478(3)	0.0706(1)	0.52(5)
P(2)	0.6277(5)	0.2662(3)	0.1760(1)	0.55(4)
P(3)	0.2403(4)	0.1393(3)	0.4348(1)	0.45(4)
P(4)	0.8671(4)	0.7106(3)	0.3223(1)	0.53(4)
O(1)	0.270(1)	0.5883(8)	0.4698(4)	1.2(2)
O(2)	0.671(1)	0.6950(6)	0.3910(3)	0.9(2)
O(3)	0.123(1)	0.7721(7)	0.3480(3)	1.1(2)
O(4)	0.496(1)	0.7979(6)	0.5431(3)	0.8(1)
O(5)	-0.054(1)	0.8620(6)	0.4951(3)	0.9(2)
O(6)	0.346(1)	0.9794(7)	0.4094(3)	0.7(2)
O(7)	0.208(1)	0.4044(8)	0.0340(4)	1.2(2)
O(8)	-0.160(1)	0.2408(6)	-0.0162(3)	0.8(1)
O(9)	0.394(1)	0.1547(7)	-0.0414(3)	0.9(2)
O(10)	0.490(1)	0.1766(6)	0.1220(3)	0.72(8)
O(11)	-0.067(1)	0.2733(7)	0.1448(3)	1.1(2)
O(12)	0.138(1)	0.0069(8)	0.0762(4)	1.0(2)
O(13)	0.312(1)	0.7683(7)	0.146(3)	1.0(2)
O(14)	0.659(1)	0.1776(7)	0.2508(3)	1.0(2)
O(15)	0.473(1)	0.4253(7)	0.1856(4)	1.0(2)
O(16)	0.103(1)	0.2352(7)	0.3703(4)	1.1(2)
O(17)	0.973(1)	0.5542(7)	0.2945(3)	1.1(2)
O(18)	0.736(1)	0.8164(7)	0.2602(4)	1.3(2)

Note. Anisotropically refined atoms are given in the form of the isotropic equivalent displacement parameter defined as $B = 4/3 \sum_i \sum_j \mathbf{a}_i \cdot \mathbf{a}_j \cdot \beta_{ij}$.

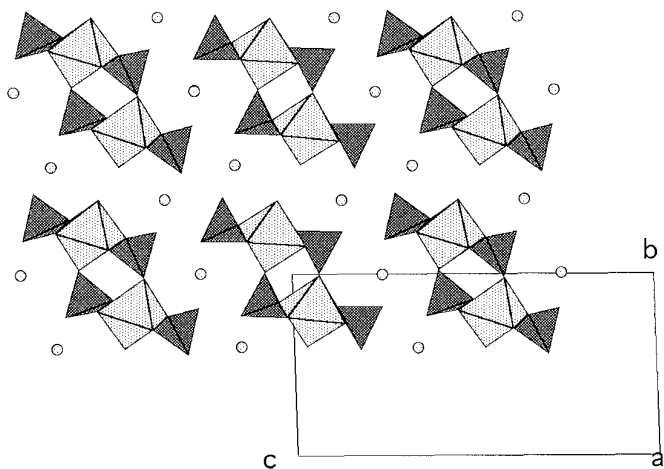


FIG. 1. Projection of the structure of Ba₃Mo₂O₂(PO₄)₂ along **a**.

they are very similar, two kinds of ribbons labeled “Mo(1)P(3)P(4)” and “Mo(2)P(1)P(2)” can be distinguished. As shown from the projection along **b** (Fig. 2) these two kinds of ribbons differ by their relative orientation; i.e., the “Mo(2)P(1)P(2)” ribbons are turned 180° around **a** with respect to the “Mo(1)P(3)P(4)” ribbons. Curiously two successive ribbons, “Mo(2)P(1)P(3)” and “Mo(1)P(3)P(4),” are approximately enantiomorphic with respect to each other, although they are not deduced one from the other by a mirror or a symmetry center. From these two projections, one observes that each ribbon [Mo₂P₄O₁₈]_∞ is built up from identical [Mo₂P₄O₁₈]_∞ chains. The projection of the [Mo₂P₄O₁₈]_∞ chains onto the (05 $\bar{1}$) plane for “Mo(2)P(1)P(2)” (Fig. 3a) and onto the (03 $\bar{1}$) plane for “Mo(3)P(3)P(4)” (Fig. 3b) shows that their geometry is very similar. In both chains, two successive MoO₆ octahedra along **c** are linked through two PO₄ tetrahedra in a similar way to that observed for KMoOP₂O₇ (5) and

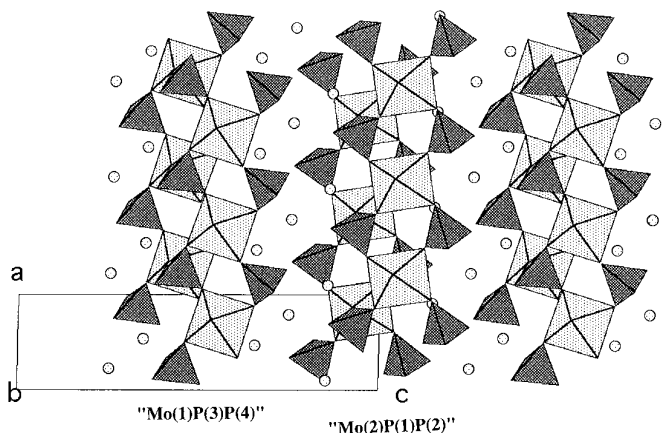


FIG. 2. Projection of the structure of Ba₃Mo₂O₂(PO₄)₂ along **b**.

TABLE 4
Distances (Å) and Angles (°) in the Polyhedra
in Ba₃Mo₂O₂(PO₄)₄

Mo(1)	O(1)	O(2)	O(3)	O(4)	O(5)	O(6)
O(1)	1.686(7)	2.680(9)	2.730(9)	2.79(1)	2.726(8)	3.80(1)
O(2)	92.3(3)	2.016(5)	2.724(8)	2.965(8)	3.963(7)	2.790(8)
O(3)	94.1(3)	84.6(2)	2.031(6)	4.025(8)	2.849(8)	2.66(1)
O(4)	97.4(3)	94.7(2)	168.5(3)	2.015(6)	2.757(8)	2.893(8)
O(5)	96.5(3)	170.5(2)	91.1(2)	87.8(2)	1.961(5)	2.785(9)
O(6)	173.3(3)	84.9(2)	79.7(3)	88.8(2)	86.0(2)	2.118(7)
Mo(2)	O(7)	O(8)	O(9)	O(10)	O(11)	O(12)
O(7)	1.682(8)	2.74(1)	2.69(1)	2.729(8)	2.73(1)	3.78(1)
O(8)	95.6(3)	2.007(6)	2.657(7)	3.995(8)	2.974(8)	2.838(8)
O(9)	93.7(3)	83.2(2)	1.996(5)	3.005(8)	4.016(8)	2.846(9)
O(10)	95.1(3)	169.3(2)	97.4(2)	2.005(5)	2.677(8)	2.692(9)
O(11)	94.2(3)	94.9(2)	172.1(3)	83.1(2)	2.030(6)	2.770(9)
O(12)	176.8(3)	87.4(2)	88.0(3)	81.9(3)	84.3(3)	2.099(7)
P(1)	O(13)	O(12) ⁱ	O(8) ⁱⁱ	O(9) ⁱⁱⁱ		
O(13)	1.509(6)	2.487(9)	2.475(8)	2.483(8)		
O(12) ⁱ	110.8(4)	1.513(7)	2.539(9)	2.846(9)		
O(8) ⁱⁱ	108.4(4)	112.3(4)	1.543(7)	2.498(9)		
O(9) ⁱⁱⁱ	108.1(3)	109.8(4)	107.3(3)	1.558(6)		
P(2)	O(10)	O(14)	O(15)	O(11) ^{iv}		
O(10)	1.545(6)	2.479(8)	2.581(9)	2.525(9)		
O(14)	107.1(4)	1.538(6)	2.527(9)	2.511(9)		
O(15)	115.1(3)	111.7(4)	1.515(7)	2.475(8)		
O(11) ^{iv}	108.3(3)	107.8(3)	106.7(4)	1.570(6)		
P(3)	O(16)	O(6) ^v	O(5) ^{vi}	O(4) ^{vii}		
O(16)	1.513(6)	2.489(9)	2.563(8)	2.483(8)		
O(6) ^v	109.4(4)	1.537(7)	2.501(8)	2.512(9)		
O(5) ^{vi}	115.2(3)	109.7(4)	1.523(6)	2.480(8)		
O(4) ^{vii}	107.5(4)	108.1(3)	106.8(3)	1.567(6)		
P(4)	O(2)	O(17)	O(18)	O(3) ^{iv}		
O(2)	1.548(6)	2.459(8)	2.595(9)	2.513(8)		
O(17)	106.4(3)	1.524(7)	2.510(9)	2.50(1)		
O(18)	115.8(3)	111.4(4)	1.515(6)	2.441(8)		
O(3) ^{iv}	108.5(3)	108.9(3)	105.7(4)	1.548(7)		
Ba(1)–O(3) ^v	2.792(6)		Ba(2)–O(1) ^{viii}	3.473(7)		
Ba(1)–O(6) ^v	2.902(6)		Ba(2)–O(1)	2.930(7)		
Ba(1)–O(10)	3.157(6)		Ba(2)–O(2)	2.979(6)		
Ba(1)–O(11)	3.186(6)		Ba(2)–O(3)	3.522(6)		
Ba(1)–O(12)	3.189(7)		Ba(2)–O(4) ^{viii}	2.725(6)		
Ba(1)–O(13) ^v	2.895(6)		Ba(2)–O(14)	2.740(6)		
Ba(1)–O(14)	2.895(7)		Ba(2)–O(15)	2.894(6)		
Ba(1)–O(14) ^{viii}	2.851(6)		Ba(2)–O(16)	2.886(7)		
Ba(1)–O(16)	3.025(7)		Ba(2)–O(16) ^{iv}	2.916(6)		
Ba(1)–O(18) ^v	2.731(6)		Ba(2)–O(17)	2.823(7)		
Ba(1)–O(18) ^{ix}	3.166(7)		Ba(2)–O(17) ^{viii}	2.931(6)		
Ba(3)–O(7) ^{iv}	2.901(7)		Symmetry codes:			
Ba(3)–O(7) ⁱⁱⁱ	3.301(7)		i: x, y + 1, z			
Ba(3)–O(8) ⁱⁱⁱ	3.076(6)		ii: –x, 1 – y, –z			
Ba(3)–O(9) ⁱⁱⁱ	3.050(6)		iii: 1 – x, 1 – y, –z			
Ba(3)–O(11) ^{iv}	2.956(7)		iv: 1 + x, y, z			
Ba(3)–O(13) ^v	2.753(7)		v: x, y – 1, z			
Ba(3)–O(13)	2.967(6)		vi: –x, 1 – y, 1 – z			
Ba(3)–O(15)	2.907(7)		vii: 1 – x, 1 – y, 1 – z			
Ba(3)–O(15) ^{iv}	2.972(6)		viii: x – 1, y, z			
Ba(3)–O(17)	2.694(6)		ix: x – 1, y – 1, z			
Ba(3)–O(18)	2.905(6)					

Note. The Mo–O or P–O distances are on the diagonal, above the diagonal are the O...O distances, and below it are the O–Mo–O or O–P–O angles.

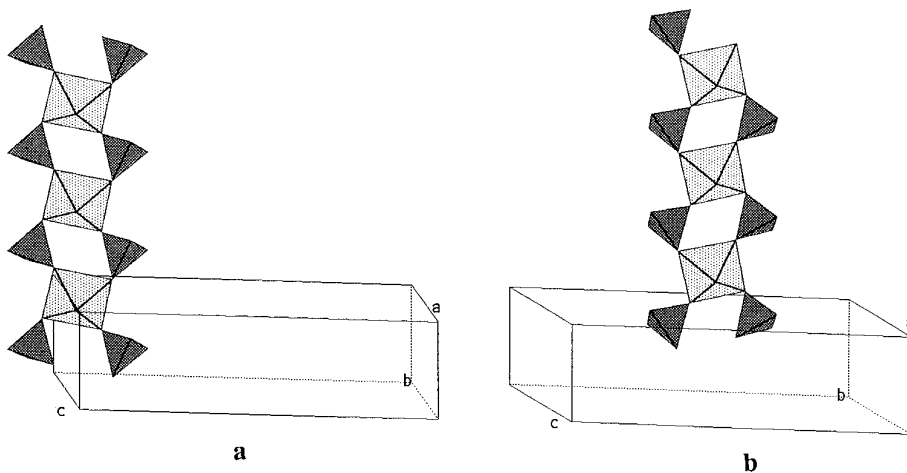


FIG. 3. (a) “Mo(2)P(1)P(2)” chain projected onto the $(05\bar{1})$ plane. (b) “Mo(1)P(3)P(4)” chain projected onto the $(03\bar{1})$ plane.

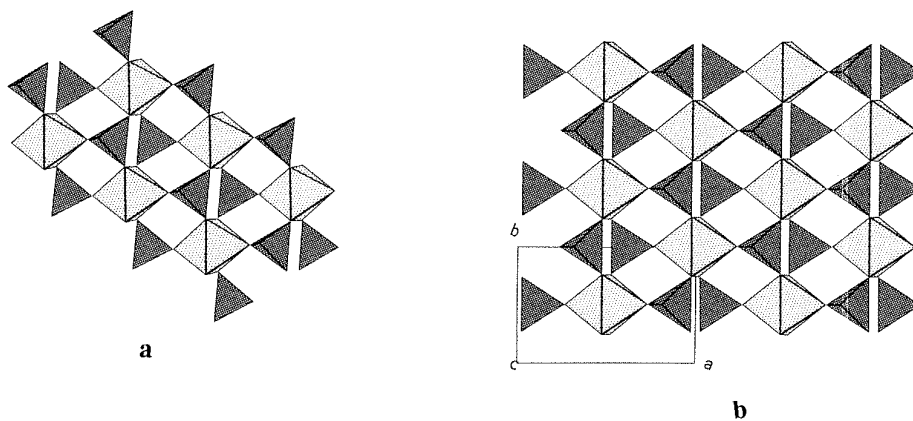


FIG. 4. (a) $\text{Mo}(1)\text{P}_4\text{O}_{18}$ ribbon projected onto the $(01\bar{4})$ plane. (b) Projection onto the (001) plane of a $\text{BaMo}(\text{PO}_4)_2$ layer.

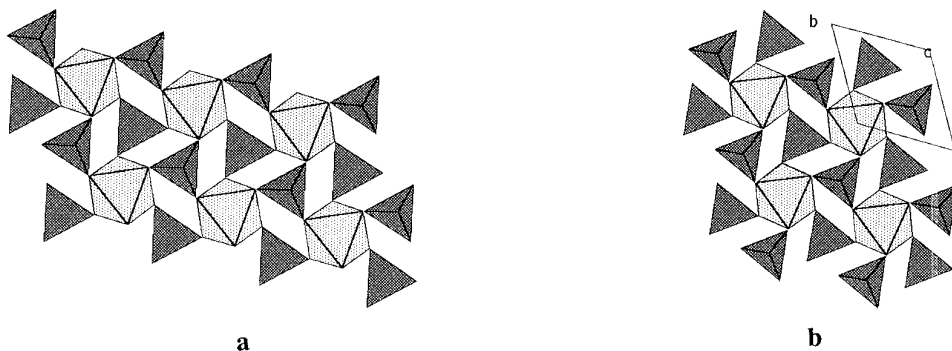


FIG. 5. (a) $\text{Mo}(2)\text{P}_4\text{O}_{18}$ ribbon projected onto the $(01\bar{4})$ plane. (b) Projection onto the (001) plane of a $\text{CsSb}(\text{PO}_4)_2$ layer.

$\text{BaMo}(\text{PO}_4)_2$ (4). This results in diamond shaped windows with O–O–O angles close to 60° – 120° in both of them.

The $[\text{Mo}_2\text{P}_4\text{O}_{18}]_\infty$ ribbons are built up of two $[\text{Mo}_2\text{P}_4\text{O}_{10}]_\infty$ chains that share the apices of their polyhedra, in such a way that an MoO_6 octahedron of one chain is linked with a tetrahedron of the second chain. As a result, in the

two kinds of $[\text{Mo}_2\text{P}_4\text{O}_{18}]_\infty$ ribbons each MoO_6 octahedron shares five apices with five PO_4 tetrahedra and exhibits one free apex characteristic of Mo(V); in the same way each PO_4 tetrahedron shares either two or three apices with the MoO_6 octahedra, so that each tetrahedron exhibits either two free apices (P(2) and P(4) tetrahedra) or one

TABLE 5
Electrostatic Valence Distribution for Ba₃Mo₂O₂(PO₄)₄

	Mo(1)	Mo(2)	P(1)	P(2)	P(3)	P(4)	Ba(1)	Ba(2)	Ba(3)	Σv _i ⁻
O(1)	1.686							0.041 0.177		1.904
O(2)	0.691					1.163		0.155		2.009
O(3)	0.663					1.163	0.257	0.036		2.119
O(4)	0.693				1.105			0.309		2.107
O(5)	0.802				1.245					2.047
O(6)	0.524				1.199		0.191			1.914
O(7)		1.704							0.192 0.065	1.961
O(8)		0.708	1.179						0.120	2.007
O(9)		0.729	1.132						0.128	1.989
O(10)		0.712		1.173			0.096			1.981
O(11)		0.665		1.096			0.089		0.165	2.015
O(12)		0.552	1.279				0.088			1.919
O(13)			1.292				1.195		0.286 0.160	1.933
O(14)				1.195			0.195 0.220	0.296		1.906
O(15)				1.272				0.195	0.189 0.158	1.814
O(16)					1.279		0.137	0.199 0.184		1.799
O(17)						1.241		0.237 0.177	0.336	1.990
O(18)						1.272	0.304 0.093		0.189	1.858
Σv _i ⁺	5.059	5.07	4.882	4.736	4.827	4.839	1.864	2.005	1.988	

free apex (P(1) and P(3) tetrahedra). The geometry of the [Mo₂P₄O₁₈]_∞ ribbons is closely related to the structure observed for the layered phosphates ASb(PO₄)₂ with A = K, Cs (6) and BaMo(PO₄)₂ (4): the “Mo(1)P(3)P(4)” ribbons are similar to the layer of CsSb(PO₄)₂ (Fig. 4) whereas the Mo(2)P(1)P(2) ribbons are similar to the BaMo(PO₄)₂ layers (Fig. 5).

The geometry of the MoO₆ octahedra and PO₄ tetrahedra (Table 4) is very similar in the two sorts of ribbons. Each “O₆” octahedron is almost regular, molybdenum being off-centered so that one observes one abnormally short Mo–O bond (1.682–1.686 Å) corresponding to the free apex, the opposite bond being long (2.118–2.099 Å); the four Mo–O distances of the basal plane of the octahedra are intermediate, ranging from 1.961 to 2.031 Å for Mo(1), and from 1.996 to 2.030 Å for Mo(2). Note that the Mo(1) octahedra are slightly more distorted than the Mo(2) octahedra.

The P–O distances (Table 4) of the PO₄ tetrahedra show that they are slightly distorted in agreement with the fact that they exhibit free apices. For each P(1) and P(3) tetrahedron one observes one shortest P–O bond (1.509–1.513 Å) corresponding to the free apex O(13) or O(16), respectively, whereas each P(2) and P(4) tetrahedron exhibits two shortest P–O bonds of 1.515–1.538 Å and 1.515–1.524

Å corresponding to two free apices, O(14), O(15) and O(17), O(18), respectively.

It is remarkable that the cohesion of such a structure is ensured by the presence of Ba²⁺ cations that sit in three kinds of sites, all characterized by an elevenfold coordination (Table 4), with Ba–O distances ranging from 2.694 to 3.473 Å. The geometry of the BaO₁₁ polyhedra is not regular. Note that for each barium atom there exist strong Ba–O bonds with the surrounding [Mo₂P₄O₁₈]_∞ chains: Ba(1) exhibits six Ba–O distances smaller than 2.90 Å, and one observes nine Ba–O distances smaller than 3 Å for Ba(2) and eight such distances for Ba(3) (Table 4).

The valences of the cations and anions have been calculated, taking into account the crystallographic results previously obtained for all the Mo(V) phosphates, using the Brese and O’Keeffe expression (7). The bond valence parameter can be refined to $R_{ij} = 1.879$ on the basis of the data obtained from 68 Mo(V) octahedra of various structures. One observes valences of the atoms in good agreement with the formal charges expected for all the atoms (Table 5). Note especially the calculated valences of 5.06 and 5.07 for Mo(1) and Mo(2), respectively, that confirm the pentavalent character of molybdenum.

In order to check the Mo(V) valence, magnetic measure-

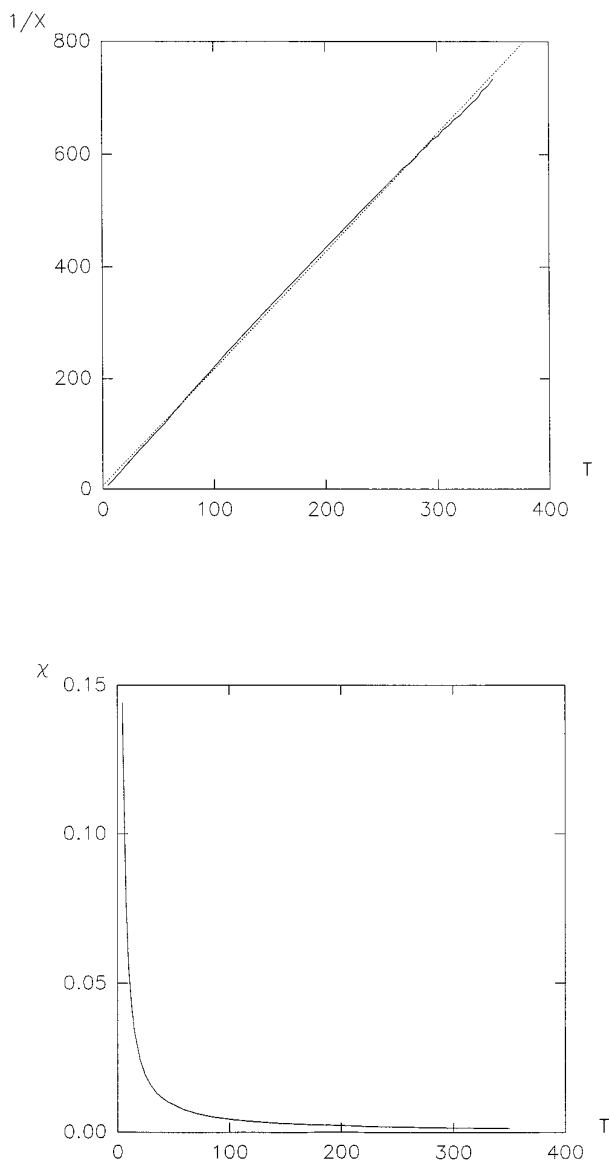


FIG. 6. The magnetic susceptibility χ and $1/\chi$ versus T for $\text{Ba}_3\text{Mo}_2\text{O}_2(\text{PO}_2)_4$.

ments were performed on a powder sample, in the temperature range from 4.5 to 350 K, with a SQUID magnetometer for an applied field B of 1 T the sample being first zero field cooled, and the magnetic field being applied after stabilization of the temperature at 4.5 K. The inverse molar susceptibility curve $\chi_M^{-1}(T)$ established after correction of the sample holder signal and the core diamagnetism shows a classical Curie–Weiss law $\chi_M = C/(T - \theta)$ (Fig. 6) leading to an effective magnetic moment of $1.88 \mu_B$ per molybdenum and to $\theta = 0.876$ K. This value, close to the theoretical moment for Mo(V) of $1.73 \mu_B$, is in agreement with the fact that all the Mo(V) octahedra are isolated, i.e., linked through PO_4 tetrahedra.

CONCLUDING REMARKS

A molybdenum(V) phosphate with a chain-like structure has been synthesized for the first time. The originality of this structure holds in the nature of the $[\text{Mo}_2\text{P}_4\text{O}_{18}]_\infty$ ribbons that are themselves built up of two corner-sharing $[\text{MoP}_2\text{O}_{10}]_\infty$ chains. It is remarkable that although one observes two kinds of crystallographically independent ribbons, these two sorts of ribbons exhibit a very similar geometry and can be considered as practically enantiomorphic.

The stability of this phase at rather high temperature suggests that it should be possible to synthesize other chain-like molybdenophosphates, in barium-rich regions of the system Ba–Mo–P–O.

REFERENCES

1. R. C. Haushalter and L. A. Mundi, *Chem. Mater.* **4**, 31 (1992).
2. G. Costentin, A. Leclaire, M. M. Borel, A. Grandin, and B. Raveau, *Rev. Inorg. Chem.* **13**, 77 (1993).
3. K. H. Lii and R. C. Haushalter, *J. Solid State Chem.* **69**, 320 (1987).
4. M. M. Borel, J. Chardon, A. Leclaire, A. Grandin, and B. Raveau, *J. Solid State Chem.* **112**, 317 (1994).
5. C. Gueho, M. M. Borel, A. Grandin, A. Leclaire, and B. Raveau, *Z. Anorg. Allg. Chem.* **615**, 104 (1992).
6. S. Oyetola, A. Verbaere, Y. Piffard, and M. Tournoux, *Eur. J. Solid State Inorg. Chem.* **25**, 259 (1988).
7. N. E. Brese and M. O'Keeffe, *Acta Crystallogr. Sect B* **47**, 192 (1991).